Reemission technique for symmetry measurements in Hohlraum targets containing a centered high-*Z* ball

N. D. Delamater, G. R. Magelssen, and A. A. Hauer
Los Alamos National Laboratory, Los Alamos, New Mexico 87544
(Received 25 October 1994; revised manuscript received 9 June 1995)

A technique for measuring time-resolved drive symmetry in a laser-irradiated *Hohlraum* is presented. Design considerations and experimental method and results are emphasized. The experimental method involves x-ray imaging a high-*Z* ball placed in the center of a laser irradiated *Hohlraum*. We will show that the reemitted x-ray image can be measured as a function of time and that the images are directly related to the radiation flux asymmetry within the *Hohlraum*. Results from a series of experiments performed on the Nova laser located at Lawrence Livermore National Laboratory will be presented as well as a method for comparing with theoretical calculations. Detailed comparisons between theoretical calculations and experimental results will be given. [S1063-651X(96)02105-1]

PACS number(s): 52.25.−b

INTRODUCTION

A critical issue in indirect drive fusion experiments is the amount of flux asymmetry seen at the target in the center of a *Hohlraum*, since too large an asymmetry would drive a distorted implosion that inhibits the attainment of high density and yield. As a result, much attention has been given to understanding and measuring symmetry within the *Hohlraum* environment [1–7]. Our ability to directly measure the time-dependent asymmetry has been greatly enhanced by recent refinements of spatially and temporally resolved imaging diagnostics that have recently become available for experiments located at the Nova laser facility at Lawrence Livermore National Laboratory. One method that has been developed to measure drive asymmetry is to image the compressed cores of imploded targets [1,2]. An inherent assumption of this method is that the final shape of the imploded core image is a direct reflection of the drive symmetry signature imprinted during the heating drive in the *Hohlraum*. Calculations agree with this assumption for the lowest-order asymmetries, but the calculations need to be benchmarked with experimental data that more directly measure time-dependent drive asymmetry. Further, the time resolution of this method is limited to the time it takes for the capsule to implode and to the observable signal strengths from the imploded core. The reemission technique is one of the recent direct approaches to the measurement of drive symmetry at the capsule location that have been applied to experiments on the Nova laser [8].

In this paper we will describe the ''reemission ball'' concept and design of drive symmetry measurement as well as experimental results from a series of experiments performed on the Nova laser facility. A method for comparing experimental results with theoretical calculations will be presented and detailed comparisons between theory and experiment will be shown.

EXPERIMENTAL CONCEPT AND DESIGN

The reemission ball is a nonimploding solid high-*Z* ball positioned at the center of a *Hohlraum*. The ball is placed at the initial position of a typical imploding capsule and samples the drive pattern at this location. The ball reemits thermal radiation under the influence of the radiation drive in the *Hohlraum*. We will show that the reemitted radiation is directly related to the incident radiation flux pattern in the *Hohlraum* center.

To show the feasibility of the concept several important issues had to be addressed. The reemitted signal had to be detectable above background emission in the *Hohlraum* (good signal-to-noise ratio) and had to be observed at a high enough photon energy to obtain good sensitivity to flux variations along the surface of the ball and still maintain strong enough signal level. Fluorescence effects had to be small. To be a measure of the radiation flux asymmetry, the reemitted image must be a measure of thermal emission, not fluorescence, caused by high energy photons from laser spot regions. There must be a simple way to compare the reemitted signals with theoretical calculations. Finally, because the *Hohlraum* fills with hot plasma, limitations of the concept needed to be addressed and understood.

An example of the *Hohlraum* target configuration used in our experiments is shown in Fig. 1. The *Hohlraum* was 2800 μm long and 800 μm in radius. The laser entrance holes were 600 μm in radius and the *Hohlraum* walls 25 μm thick. On each side of the *Hohlraum*, five laser beams entered the *Hohlraum* through the entrance holes and created a five spot

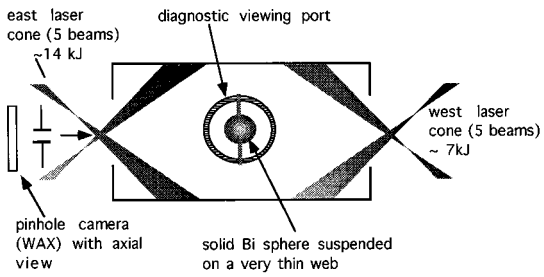

FIG. 1. Experimental configuration showing x-ray diagnostic locations.

ring pattern on the *Hohlraum* walls. The reemission ball was placed in the center of the *Hohlraum*, replacing the standard 550-μm-diam plastic capsule [1]. The ball was solid bismuth 300–360 μm in diameter. Bismuth balls were chosen because they were easy to fabricate, because they are a high-Z material and because their m-line emission did not overlap with gold. The diagnostic hole viewing perpendicular to the *Hohlraum* axis was 700 μm in diameter to allow a good image of the bismuth ball for at least 1 ns. To try to avoid problems associated with the ball mounting mechanism, the ball was held with two thin 700 Å thick plastic sheets placed perpendicular to the *Hohlraum* axis. The emission from laser spots, the most intense source of x rays above 1 keV inside the *Hohlraum*, can create problems in understanding the image from the bismuth ball. To eliminate the rear wall laser spot emission problem a 800-μm-diam hole was placed opposite the 700-μm viewing port. Appropriate filtering of the x-ray imager is also critical for achieving good results in these experiments. In our experiments filtering much below 1 keV makes the technique too insensitive to asymmetries. On the other hand, if the filter is at too high of an energy the signal is too weak and is dominated by noise. For the experiments presented, the best filter was 150 μm of Be, which gives a peak between 2 and 3 keV. The laser pointing (the center point where the five Nova laser beams cross) was located along the *Hohlraum* axis at the laser entrance hole or 50 μm outside of it. This pointing location kept the laser hot spots far from the viewing ports.

Because of the difficulties experienced in earlier experiments [9–12], our first experiments had a large 2:1 west-east beam imbalance to reduce the possibility of not being able to measure a good signal and an asymmetry effect from the ball. Subsequent experiments were performed to test the sensitivity of the technique. These tests were done by progressively lowering the beam imbalance from 2:1 to 1:1. Using equal east-west energies allows the study of just the pole-to-equator asymmetry caused by the location of the laser beam spots on the *Hohlraum* wall [1].

The x-ray image of the ball was measured using the gated x-ray imager (GXI) developed at Los Alamos [13–15]. The GXI is a gated microchannel plate, multiple pinhole camera with both time and space resolution. The gating of the microchannel plate produces a series of snapshot frames of about 80-ps duration. For our shots the temporal resolution was about 50 ps and spatial resolution was about 20 μm. The GXI camera was pointed perpendicular to the *Hohlraum* axis and viewed through the 700-μm-diam diagnostic hole. Another time and spatially resolved pinhole camera using similar technology, WAX [16], viewed along the *Hohlraum* axis. The GXI data showed the effects of the east-west beam imbalance and the WAX data showed the three-dimensional (3D) effects of the individual beam imbalances azimuthally around the ball.

The *Hohlraum* was illuminated with the ten Nova laser beams using a 1-ns square laser pulse with 20–27 kJ of laser energy. Again, the experimental configuration and diagnostics are shown in Fig. 1. Time-resolved x-ray images of the ball in the direction perpendicular to the *Hohlraum* axis were obtained from the GXI data and the time development in the azimuthal direction was obtained from the WAX data. The images were analyzed using the data analysis computer code

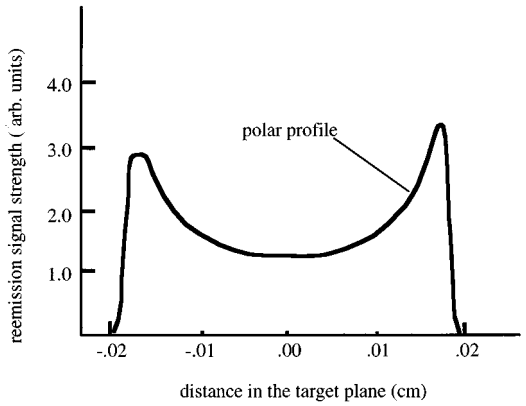

FIG. 2. Calculated lineouts of horizontal images of the ball.

PDSSHRINK [17]. The raw film density data were converted to exposure using a calibrated wedge. The image in exposure units was then filtered by a median filter to eliminate noise spikes introduced from the microchannel plate in the GXI. By taking horizontal lineouts through the center of each image, the polar signal ratio was obtained and could be plotted as a function of time.

THEORETICAL MODELING

To understand the relationship between reemitted image from the ball and incident radiation flux asymmetry, a series of 2D LASNEX [2,3,9] calculations were performed to determine if a given flux asymmetry created a unique signature from the ball. The radiation physics from the ball was done both local thermodynamic equilibrium (LTE) and non-local thermodynamic equilibrium (NLTE). The ball emission image was the same for these two different types of radiation physics. The images presented here are for the NLTE calculations. To study the ball emission image, a constant pole-to-pole ($P1$) radiation flux asymmetry was applied. The radiation source was multigroup and time dependent. It was created by doing a 2D LASNEX *Hohlraum* calculations without the ball with 20–25 kJ and 1-ns laser source profile. For this amount of laser energy the *Hohlraum* radiation temperature is above 200 eV for most of the pulse. To obtain an image that can be compared with experimental results, the LASNEX result is post processed. The post processor uses a sequence of snapshots from LASNEX calculations to determine the time-dependent emission seen by the detector from the ball. For each snapshot the post processor does a detailed ray-trace radiation transport calculation from the ball to the detector. The detector had a flat filter allowing all photons above 2 keV to produce the image. Figure 2 shows a 50-μm-width lineout of the ball image taken along the polar axis (*Hohlraum* axis). The difference in the east-west signal peaks is indicative of the amount of east-west asymmetry. The ratio of these two peaks is what we use to monitor the asymmetry. For a constant east-west source asymmetry, the peak pole-to-pole signal ratio was studied as a function of time. Examples of the time dependence of the signal ratios for constant east-west ($P1$) incident flux asymmetries are shown in Fig. 3. The examples are for 18% and 27% flux asymmetries. Notice that after the first 100 ps, the signal ratio remains almost constant, decreasing slightly with time

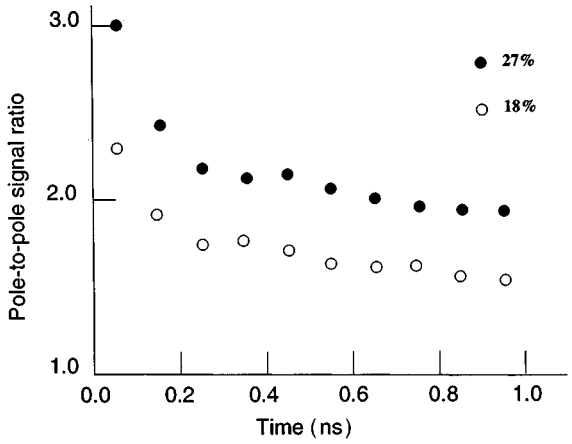

FIG. 3. Time dependence of the signal ratio for a constant 18% and 27% radiation flux.

and varying about 10%. This is typical of the results for other constant flux asymmetries. The averaged signal ratio values (excluding the first 100 ps) for $P1$ flux asymmetries of 5%, 10%, and 15% were 1.16, 1.35, and 1.55, respectively. Furthermore, more complex asymmetries were given as input to the LASNEX calculation and in every case there was a one-to-one correspondence between signal ratios and incident flux pattern. Our comparisons between calculations and experimental data will illustrate the one-to-one correspondence.

To understand the results displayed in Fig. 3, consider two different limits. If the ball were a perfect blackbody radiator without motion (albedo of one), a given incident flux asymmetry would create an identical emitted flux pattern. For example, the incident radiation temperature and the ball electron temperature would be the same and therefore the emitted radiation would be a reflection of the incident radiation. On the other hand, if the ball had an albedo of zero, the ball would not radiate. The incident radiation would couple only to the ball plasma hydrodynamics and internal energy.

Experimentally, the two extremes are represented by high-Z and low-Z ball materials. For example, if the ball were made of lithium, the absorption region would quickly become fully ionized and the ball would weakly radiate (low albedo). The incoming radiation would couple mostly to plasma motion and internal energy and decouple from the electron temperature. As a result, the incident and emitted radiation decouple.

In our experiments bismuth is used for the ball material because it is close to a black-body radiator. Only during the first 100–150 ps is the bismuth albedo low. After this short period the albedo reaches values near 0.8 to more than 0.9 late in the laser pulse. The ball absorbs radiation and motion occurs. However, most of the incident radiation is reemitted and a growing electron temperature difference does not occur. For example, electron temperature buildup in the hotter region does not occur. Further, the difference in hydrodynamic motion is small because the difference in temperature is typically less than 5%. Our calculations indicate that the electron temperature difference remains approximately the

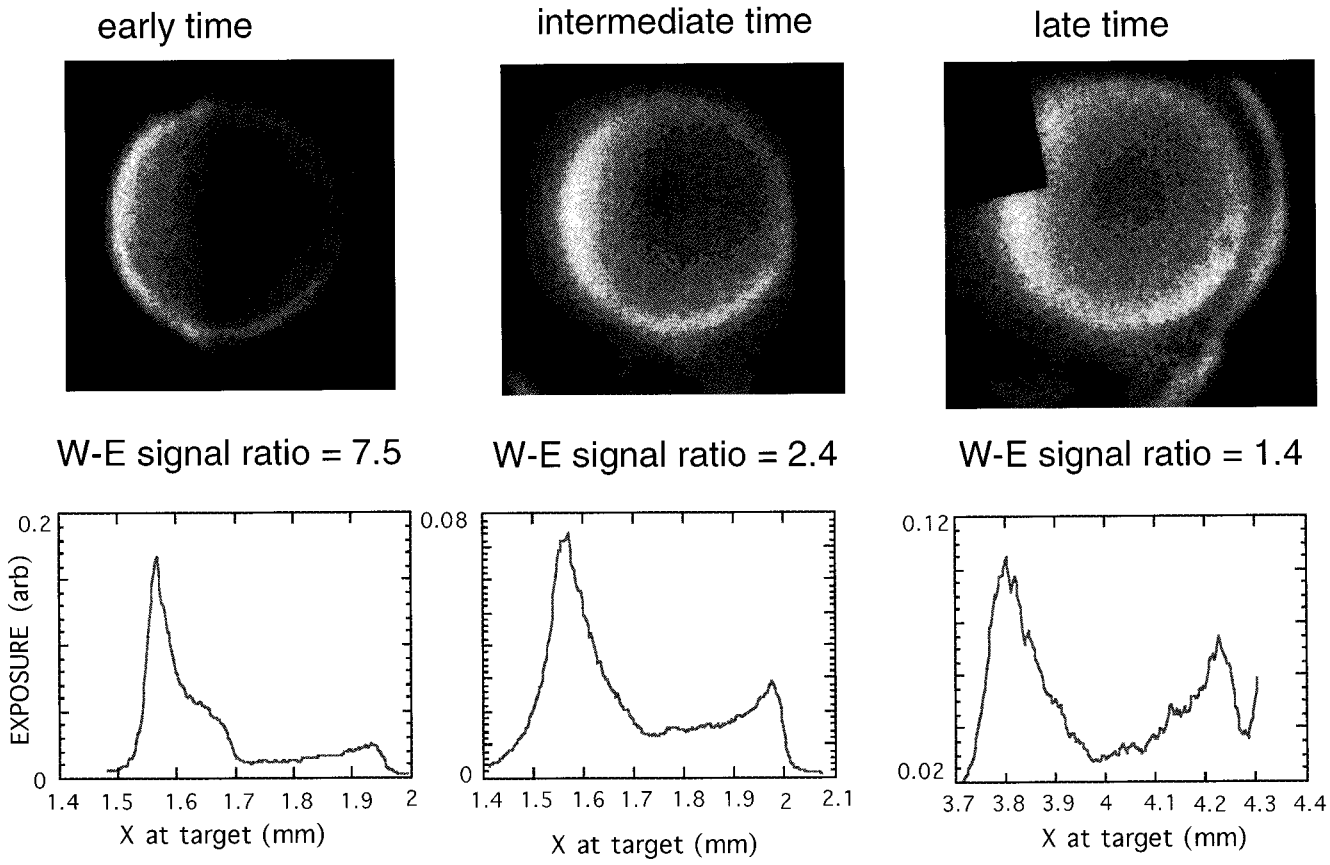

FIG. 4. Experimental images for the 2:1 west-east beam imbalance.

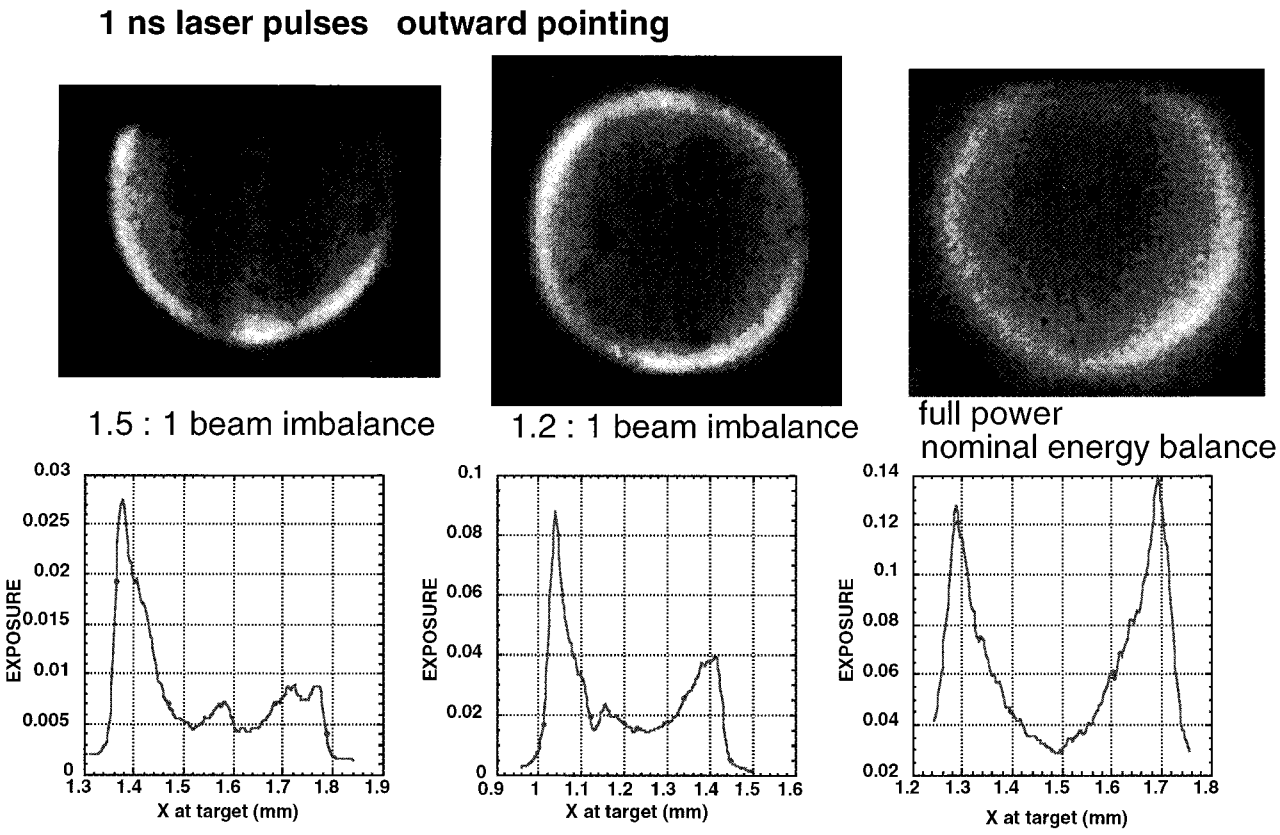

FIG. 5. Experimental images for different west-east beam imbalances.

same as the incident radiation temperature difference. For these reasons the signal ratio remains approximately constant for a constant incident flux. For more general situations, this high albedo creates the one-to-one correspondence between incident and emitted flux.

EXPERIMENTAL RESULTS

Our first shots that had a deliberately large 2:1 west-east laser energy imbalance are depicted in Fig. 4. The GXI images are shown as well as 50-μm-wide polar lineouts through the center of each image. Notice that these images are similar to those shown in Fig. 2. The lineouts shown in Fig. 4 are for 0.15, 0.50, and 0.75 ns during the 1-ns laser pulse. The GXI was filtered with 6 ml of Be, which, combined with the spectral response of the microchannel plate detector, gave a peak response to x rays in the range of 2–3 keV photon energy. The images give a characteristic ''half or crescent moon'' effect due to the large beam energy imbalance. The images from this shot also show 3D effects due to a random beam imbalance in the up-down direction. Note that the image of the reemission ball is quite distinct and seen with a good signal-to-noise ratio. The late time image shows evidence of expansion due to emission from the hot blowoff plasma and the ball has expanded close to the diagnostic hole, which is also visible. These experiments clearly illustrate the feasibility of the obtaining and measuring ball emission signals with a good signal-to-noise ratio. By using the appropriate filtering, by avoiding imaging *Hohlraum* walls and laser hot spots and by using bismuth balls many of the problems were overcome. Furthermore, the images are similar to those predicted by calculations and allow direct comparison with theoretical results.

Subsequent shots were done to test the sensitivity of this technique by progressively lowering the east-west beam imbalance. For these shots, the initial beam imbalance was 1.5:1, 1.2:1, and 1:1 or a ''nominal'' energy balance. We compare the GXI images at early time (150 ps) from these three different shots in Fig. 5. The figure also shows horizontal lineouts taken through the center of the ball. It is clear from these results that the reemission from the ball is sensitive to the initial beam imbalance since the lineouts show a clear difference in these three cases. For example, the 1.5:1 beam imbalance gives the largest east-west peak signal ratio while the nominal energy balance case gives almost equal peak ratios.

As has been demonstrated in implosion experiments [2], moving the five beam laser bundles along the *Hohlraum* axis changes the drive on the ball from pole hot (beams outward near the laser entrance ports) to equator hot (beams inward near the capsule). We expect the emission from the reemission ball to reflect this situation. If we look at the time-dependent GXI image data from the shot with 1.2:1 initial beam imbalance we see the evidence of the initial $P1$ (east-west) beam imbalance especially at early time, but we also see the effects of the outward pointing, which gives a $P2$ asymmetry at the ball with a large pole-to-equator flux ratio developing at later time. This trend is shown in Fig. 6, which gives the GXI images and corresponding horizontal lineouts for early, intermediate, and late time. Note that at early time

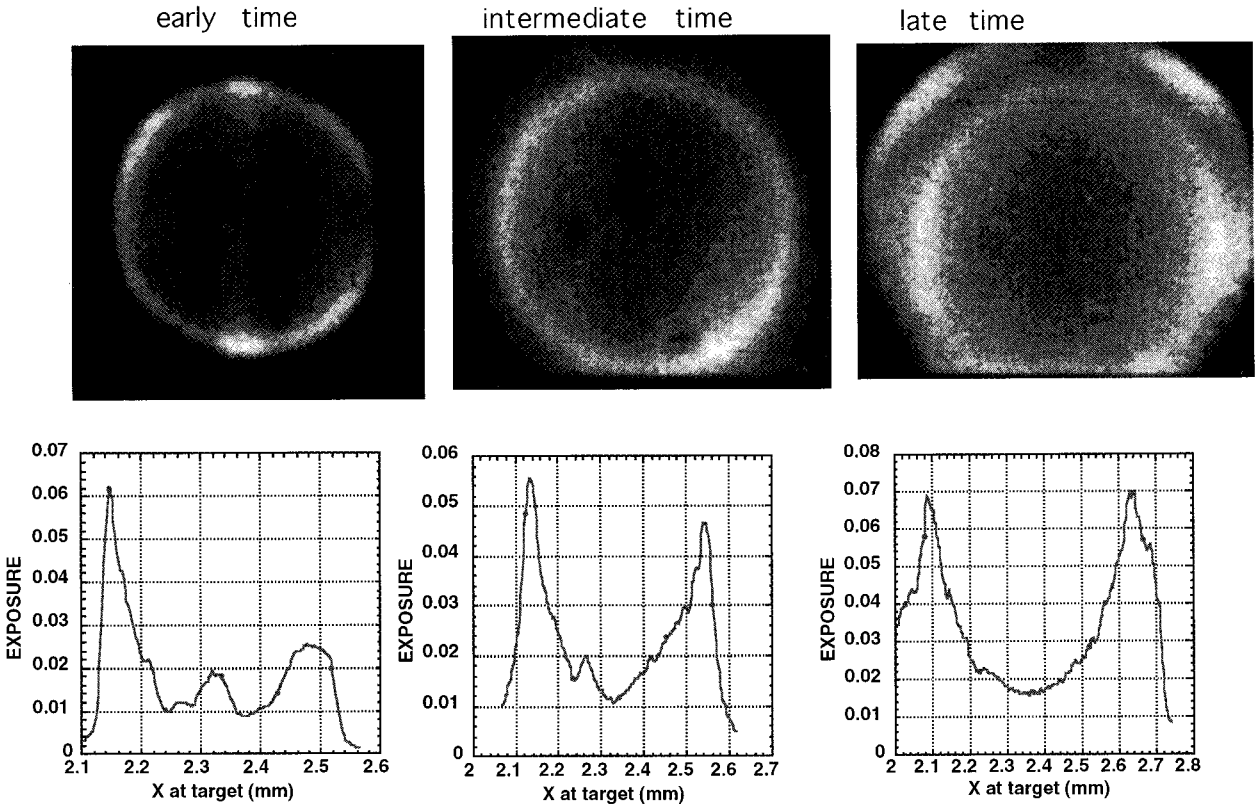

FIG. 6. Experimental images for the 1.2:1 west-east beam imbalance.

the $P1$ asymmetry dominates, but at late time the $P2$ asymmetry dominates and clear evidence is seen of the characteristic hot pole emission due to outward pointing.

The axial pinhole camera (WAX) data showed that the reemission ball at early times can detect the pattern of the individual distinct laser beams in azimuthal direction. An analysis of an early time WAX image is shown in Fig. 7. The image shows peaks in emission azimuthally around the ball, which are shown graphically in an azimuthal lineout. The angular positions of the laser beams are indicated in the figure. The correspondence is very good: the indications are that the five peaks correspond to the five pairs of beam positions in the laser beam pattern. The fact that the WAX image senses the laser beams is significant because it indicates the sensitivity of the technique.

The question of possible fluorescence was tested experimentally with the result that we believe fluorescence is not a factor for our experiments. If fluorescence were significant it would mean that the reemission ball is not emitting thermal radiation but rather is sensitive to laser hot spots and not an indicator of drive symmetry. We tested for fluorescence by coating half the reemission ball with a thin (7-μm) layer of

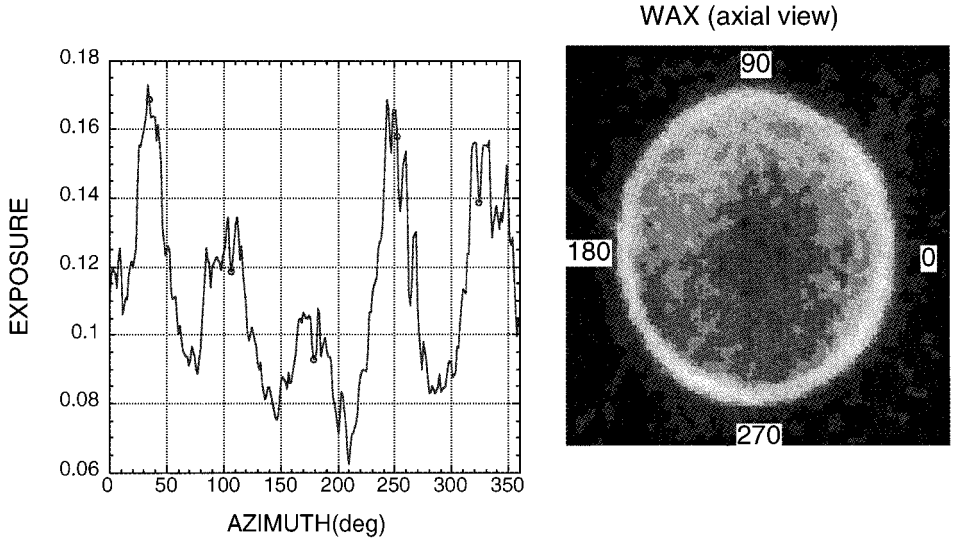

FIG. 7. Experimental images from the ball taken along the *Hohlraum* axis of the five laser spots.

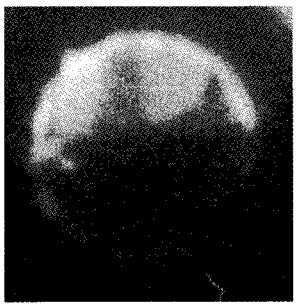

early time image of ball which is half-coated with thin layer of Be shows no emission from the coated half

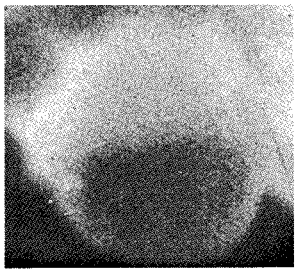

the late time image of the ball shows more uniform emission as the Be layer has burned through

FIG. 8. Measurements of the effect of fluorescence.

Be and measured the GXI time-dependent images. The result is shown in Fig. 8. The early time image of the half-coated ball shows no emission from the coated half, as would be expected if fluorescence were not important, since the high energy fluorescent emission would pass through the thin Be layer with little or no absorption. At later time, when the Be has begun to burn through, the image of the ball shows more uniform emission.

THEORETICAL COMPARISONS WITH EXPERIMENTAL RESULTS

Our theoretical approach was to use 2D fully integrated LASNEX calculations to compare with experimental results. These calculations include laser interaction with the *Hohlraum* walls, hydrodynamic motion of the walls and ball, and radiation emission and absorption everywhere within the *Hohlraum*. Two different Seame equations of state [18] for gold were used and gave identical results. NLTE radiation atomic physics [19] is used for the wall and for the ball using the average atom atomic physics package in LASNEX. To determine the effect of NLTE emission from the ball, integrated calculations with the *Hohlraum* walls NLTE and the ball LTE were also done. The calculated ball signals were the same for NLTE and LTE radiation physics. To obtain an image to compare with experimental results, the LASNEX results were post processed. The post processor uses a sequence of snapshots from LASNEX calculations to determine the time-dependent emission seen by the detector from the ball. For each snapshot the post processor does a detailed radiation transport calculation from the ball to the detector. The detector had a filter equivalent to 6 ml of Be, the filter used in the experiment. A flat filter allowing all photons above 2 keV gives a similar image with the same peak signal ratios. Our calculations are compared with three different experiments.

Our first comparison is with the experiment with a large 2:1 west-east beam imbalance. The total laser energy for this experiment was about 21.1 kJ: 7.5 kJ from the east and 13.6 kJ from the west. The west-east averaged laser power profile is shown in Fig. 9. Figure 10 gives a 50-μm-wide lineout of the ball image taken along the polar axis (*Hohlraum* axis) from a post processed LASNEX calculation for the laser and *Hohlraum* conditions of this experiment. The lineout is time integrated over the first 100 ps of the laser pulse and the image is filtered with 6 ml of Be. This lineout is very similar to the one shown for early time in Fig. 4 for the experiment. To make a detailed comparison, the peak west-east signal ratios for the experiment and calculation are given in Fig. 11. The error in the amplitude of the experimental signal ratio is about 5%. The uncertainty in time is about 50 ps. These were the amplitude and timing uncertainties for all the results presented here. The experimental and theoretical results agree to within about 10% for all time.

Figure 12 shows the experimental and theoretical signal ratios as a function of time for the shot with initial beam imbalance of 1.2 to 1. Our analysis of the relationship be-

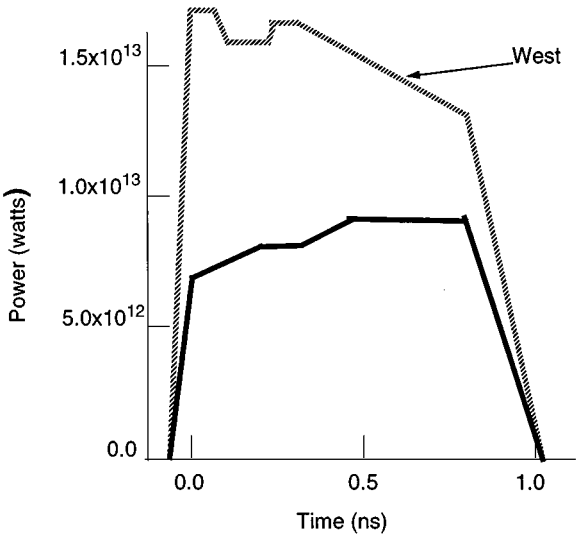

FIG. 9. West-east averaged laser power profile for the 2:1 power imbalance experiment.

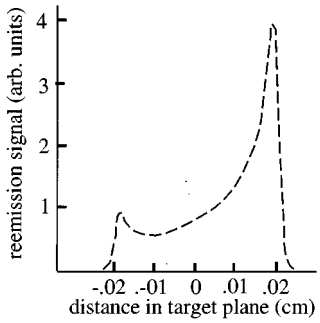

FIG. 10. Early time calculated horizontal lineout for the 2:1 west-east beam imbalance experiment.

tween peak signal ratios and flux asymmetry suggests that the flux asymmetry is varying by more than 20% (signal ratio of 2.6) to less than 5% (signal ratio of 1.05). Calculation 1 was done using the east and west averaged experimental laser intensity profiles shown in Fig. 13 and the agreement with experimental results was within 10%. If we assume a constant flat top laser profile with 100-ps rise and fall time, the calculation and experimental result disagree by as much as 100% at early time. This is shown in calculation 2. The initial large difference in west-east laser power (35% difference) as well as the late time power equilibration is clearly evident in both calculation 1 and the experimental result.

Our final comparison illustrates some of the limitations of the concept and the design and suggests future directions. In this experiment there was no west-east power imbalance. The purpose was to measure the effect of the laser pointing (P2). For example, moving the five beam laser bundles along the *Hohlraum* axis changes the drive on the ball from pole hot (beams outward near the laser entrance ports) to equator hot (beams inward near the capsule). The laser energy was 27 kJ and the laser pointing was outward near the laser entrance hole. The laser beams crossed the *Hohlraum* axis about 1350 μm from the center of the ball and therefore should create a pole hot asymmetry. The *Hohlraum* parameters were those discussed earlier. Figure 14 shows a comparison between our calculations and the experimental results. Plotted are the pole-to-equator peak signal ratios as a function of time. For the first 200–300 ps the experiment shows an equator hot asymmetry whereas the calculation gives a pole hot asymmetry. Theory and experiment agree from 300 to about 700 ps. At this time the calculated peak signal ratio becomes very large (greater than 10). At about 700 ps, the wall plasma is stagnating against the plasma blowoff from the bismuth ball. This calculated stagnation causes the large increase in the peak signal ratio. Experimentally, there is a increase in the rising slope of the peak signal ratio, but at least a factor of 10 less than calculated.

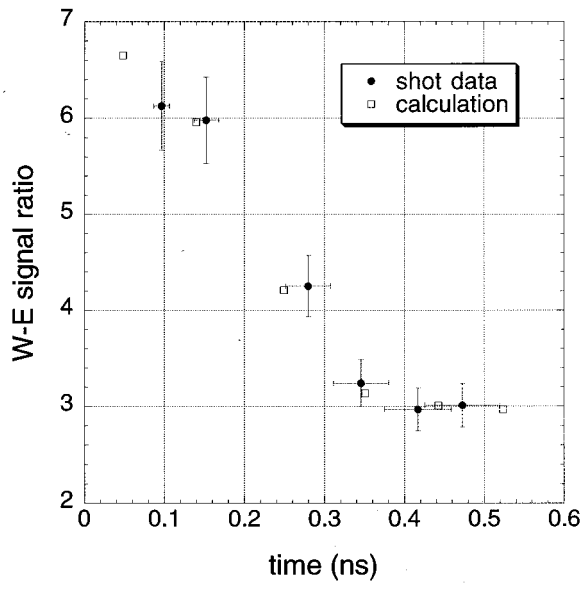

FIG. 11. Theoretical and experimental peak signal ratios plotted as a function of time for the 2:1 west-east beam imbalance experiment.

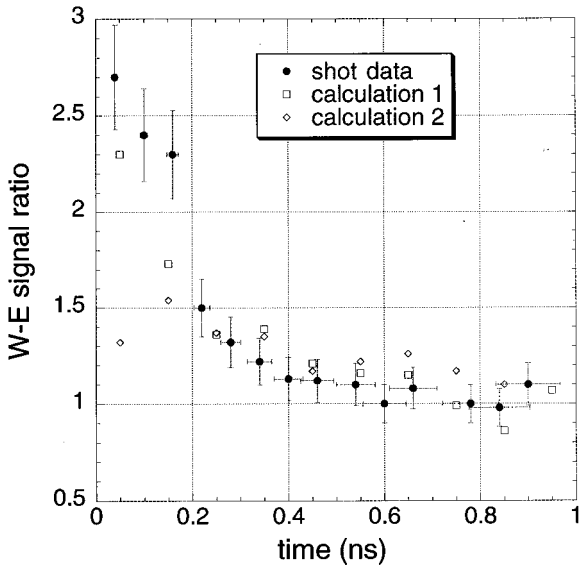

FIG. 12. Theoretical and experimental peak signal ratios plotted as a function of time for the 1.2:1 west-east beam imbalance experiment.

Our calculations do not include the thin plastic sheets

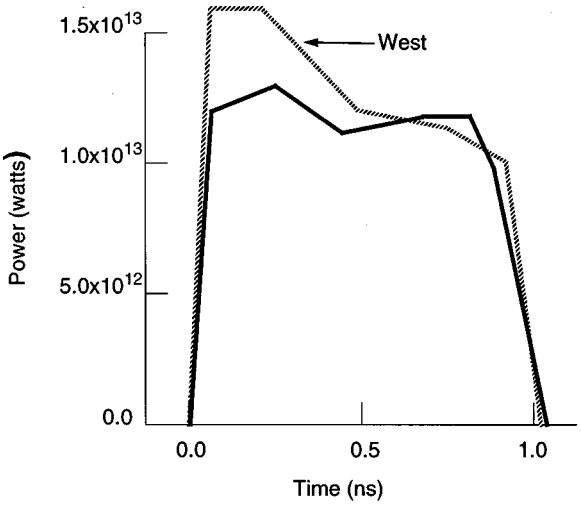

FIG. 13. Laser time-dependent profiles for the 1.2:1 experiment.

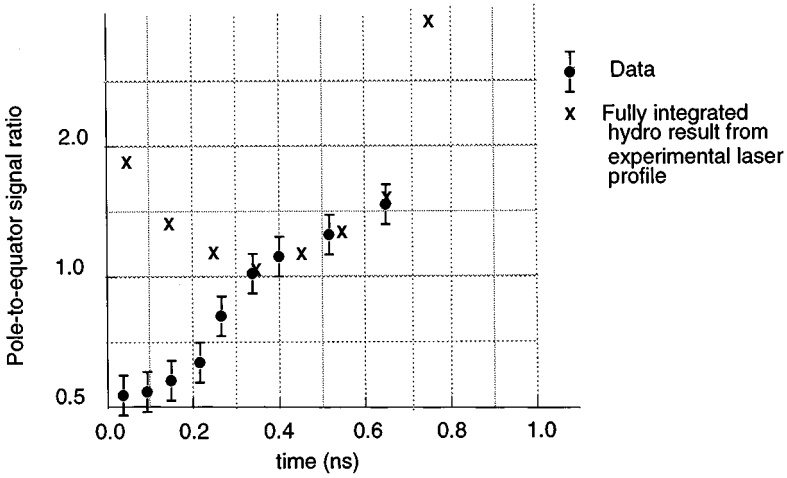

FIG. 14. For these results, the west-east directions were energy balanced. The results illustrate the impact of the position of the laser rings (outward) giving a pole-to-equator asymmetry (pole hot). They also illustrate the negative effect of the web mounting mechanism, an effect that causes large disagreements between theory and experiment at early times.

used to mount the ball in the center of the *Hohlraum*. The sheets are located in the equatorial plane of the ball and can effect the emission in this region. The signal that is seen can be affected in at least two ways. At early times before significant expansion of the sheet, x-ray emission will come from the sheet as well as the ball. Further, all regions except the equatorial area will have a layer of plastic tamping the hydrodynamic expansion of the bismuth. This could effect the bismuth emission in the equatorial plane. To avoid this problem, future experiments that study the pole-to-equator asymmetry will use a thin stalk (less than 10 μm in diameter) as a mounting mechanism.

Plasma wall filling does limit the time we can view the ball image and this effect is clearly illustrated in our experimental data and calculated results. Therefore, the technique is good for studying the early time asymmetry in vacuum *Hohlraums*. If the *Hohlraum* is filled with gas, the filling is slowed [5] and the technique might work for a much longer time.

CONCLUSIONS AND FUTURE PLANS

We have shown that the reemission ball design is an effective technique for measuring time-resolved drive symmetry in laser-irradiated *Hohlraums*. The reemitted signal is detectable above background emission in the *Hohlraum* (good signal-to-noise ratios) and is observed at a high enough photon energy to obtain good sensitivity to flux variations along the surface of the ball and still maintain strong enough signal level. Fluorescence effects are shown to be small. Theoretical calculations have illustrated the relationship between peak signal ratios and radiation flux asymmetry. Detailed comparisons between calculations and experimental results have been made and are in good agreement. Limitations of the design due to the mounting mechanism have been identified and its affect on the ball signal ratios determined. Finally, limitations on the usefulness for the concept have been illustrated both theoretically and experimentally. Because of plasma filling inside the *Hohlraum*, the technique is viable at early time, before the wall plasma collides with the ball.

Our future plans include extending this technique to study drive asymmetry in *Hohlraums* using longer shaped laser pulses. This is to study the low power portion of the drive. Calculated time-dependent asymmetries with small change in laser pointing show pole-to-equator signal ratios differing considerably initially and converging to small values. Thus the pointing studies will be used to determine the technique's sensitivity to flux asymmetry. Because of the interest in gas-filled *Hohlraums*, some future experiments will explore the usefulness of the reemission technique in the gas-filled environment. In a future paper, a general approach to relating radiation flux asymmetry and signal ratios is planned to be developed. Because of the problems with the thin film mounting mechanism, the mechanism will be replaced with a small (less than 10 μm in diameter) supporting carbon stalk in future experiments requiring measurements of the very early time asymmetry.

The results of these experiments are quite useful as benchmarks and in validating our code modeling. It is in fact one of the first times that time-dependent symmetry data has been used to verify the 2D integrated code modeling.

ACKNOWLEDGMENTS

We would like to acknowledge the LANL target fabrication group, which includes L. Foreman, P. Gobby, V. Gomez, J. Moore, and K. Gifford, for their efforts in making and assembling the reemission targets. The authors acknowledge the able technical assistance of S. Evans, T. Sedillo, T. Archuleta, and G. Peterson. The authors would like to acknowledge the assistance of L. Suter, D. Harris, G. Pollack, and R. Turner for useful discussions on the experimental design. We also acknowledge the assistance of R. Ehrlich for assistance with the production of precision energy balance on the Nova laser. We would also like to acknowledge the assistance of personnel at the Nova laser facility at the Lawrence Livermore National Laboratory. This work was performed under the auspices of the U.S. Department of Energy.

[1] A. A. Hauer *et al.*, Rev. Sci. Instrum. **66**, 672 (1995).
[2] L. J. Suter *et al.*, Phys. Rev. Lett. **73**, 2328 (1994).
[3] E. L. Lindman *et al.*, in *Proceedings of Plasma Physics and Controlled Nuclear Fusion Research, Oxford, 1994*, edited by S. J. Rose (IAEA, Vienna, 1995).
[4] E. L. Lindman *et al.*, in *Proceedings of the XIIth International Conference on Laser Interaction and Related Phenomena, Osaka, 1995*, edited by G. Miley (AIP Press, New York, 1996).
[5] N. D. Delamater *et al.*, in *Proceedings of the XIIth International Conference on Laser Interaction and Related Phenomena* (Ref. [4]).
[6] C. Stockl and G. D. Tsakiris, Phys. Rev. Lett. **70**, 943 (1993).
[7] M. Murakami and J. Meyer-Ter-Vehn, Nucl. Fusion **31**, 1333 (1991).
[8] Amendt *et al.*, Rev. Sci. Instrum. **66**, 785 (1995).
[9] Magelssen *et al.*, Defense Res. Rev. **6**, 59 (1994).
[10] Magelssen *et al.*, Los Alamos National Laboratory Report No. LA-CP-93-0078, 1993 (unpublished).
[11] R. E. Turner and L. J. Suter, Lawrence Livermore National Laboratory Report No. UCRL-50055-86/87, p. 4, 1988 (unpublished).
[12] L. J. Suter, Lawrence Livermore National Laboratory Report No. UCRL-50055-84, 1985 (unpublished).
[13] J. Oertel, R. E. Chrien, and J. M. Mack, in *Proceedings of the XIVth International Conference on Plasma Physics and Controlled Nuclear Fusion Research* (IAEA, Vienna, 1993).
[14] J. D. Kilkenny *et al.*, Rev. Sci. Instrum. **59**, 1793 (1988).
[15] D. K. Bradley *et al.*, Rev. Sci. Instrum. **63**, 4813 (1992).
[16] O. L. Landen *et al.*, SPIE Proc. **2002**, 2 (1993).
[17] D. W. Phillion (private communication).
[18] G. I. Kerley, J. Chem. Phys. **73**, 469 (1980); **73**, 478 (1980).
[19] G. Pollak, Los Alamos National Laboratory Report No. LA-UR-90-2423, 1990 (unpublished).